

3D dynamic fault sealing capacity modelling to improve history matching: a case study in Oligocene reservoir, Tay Ho Field, Blocks A, Cuu Long basin, Offshore Vietnam



Hung Viet Vu *, Dong Duc Nguyen, Gia Phuoc Phan, Vu Minh Le, Hai Hoang Ninh

PVEP Block 01/97&02/97, HCM City, Vietnam

ARTICLE INFO

Article history:

Received 19th July 2022

Revised 23rd Oct. 2022

Accepted 21st Nov. 2022

Keywords:

3D fault seal capacity,
Fault clay,
Fault permeability,
Fault thickness,
Fault transmissibility.

ABSTRACT

Fault transmissibility multipliers are a simple way of accounting for the effects of faults on fluid flow across fault plans in history matching of production simulation models. Fault transmissibility multipliers can be calculated using parameters such as fault clay, fault smear, thickness, and permeability. In this study, three empirical methods given by Manzocchi et al. (1999), Jolley et al. (2007), and Sperrevik et al. (2002) have been applied to the Oligocene sandstone reservoir, Tay Ho Field. The Oligocene reservoir is a complicated sandstone that was deposited in alluvial-fluvial and lacustrine environments, trapped by both stratigraphic and structural types, sandbody isolated by multi-activated faults. Fault sealing is one of the key factors controlling hydrocarbon accumulations and trap volume and can have a significant influence on reservoir performance during production. Furthermore, the prospective of structural or combination traps in stacked clastic reservoir settings that are typically found in many of the known hydrocarbon provinces in the Cuu Long basin, often critically hinges on the presence of a working fault side seal. Based on a thorough understanding of the key controls on fault seal risk and retention capacity, a consistent methodology to access these factors across a prospect portfolio is essential to achieve a balanced prospect ranking and an accurate assessment of prospect success volumes. In the process workflow built by PVEP Blocks 01/97 & 02/97, the assessment of fault seal capacity and compartmentalization in the Oligocene reservoir have been incorporated by using fault deformation, displacement, juxtaposition, fault zone thickness, shale gouge ratio (SGR), shale smear factor (SSF), clay smear potential (CSP), fault thickness and permeability. In our research, the Sperrevik et al. (2002) method provides the best historical match and most logical geological evidence; thus, it shall be used for dynamic models and further studies.

Copyright © 2023 Hanoi University of Mining and Geology. All rights reserved.

*Corresponding author

E - mail: hungvv1@pvep.com.vn

DOI: 10.46326/JMES.2023.64(1).06

1. Introduction

Tay Ho structure is a part of the Amethyst High Trend and located on along the north-eastern margin of the Cuu Long basin. The Oligocene Sandstone is the biggest reservoir in Tay Ho field with HIIP accounted up to 71.1 MMbbls, but its oil production had been impacted by gas cap and low-pressure maintenance. The Oligocene reservoir is complicated sandstones deposited in alluvial-fluvial and lacustrine environments, trapped by both stratigraphic and structure types. Sand body is isolated by multi activated- fault, therefore, fault transmissibility across the fault plain plays important roles for improving history matching and remaining hydrocarbon in each segment for infilled development wells as well as water injection strategy.

Play types in most of the fault bounded structural traps are associated with faults, and faults can be either sealing or conduit to fluid flow (Sahoo et al., 2010). Fault sealing is one of the key factors controlling hydrocarbon accumulations, trap volume, and can be a significant influence on reservoir performance during production. The ability to predict the impact of faults on locating remaining hydrocarbon is critical to optimal well placement.

This study presents the assessment of fault seal capacity and compartmentalization in the Oligocene reservoir by analyzing fault characteristic and deformation, fault seal capacity

parameter such as fault displacement, juxtaposition, fault zone thickness, Shale Gouge Ratio (SGR), Shale Smear Factor (SSF), Clay Smear Potential (CSP), fault plane profile (FPP), and applying the evaluation results on dynamic simulation for history matching.

2. 3D Fault seal analysis methodology and workflow

Methodology for the quantitative assessment of the impact of faults on fluid flow in petroleum reservoirs can be describe by the steps as below.

2.1. Fault zone deformation process

The fault zone deformation is dependent on sand juxtaposition process, which might occur for numerous reasons. For example, fault zone deformation can be caused by either clay smear, fault zone diagenesis, grain sliding, cataclasis and so on. Because of the characteristic of fault zone deformation, there are multiple hypothesis on how the fault zone deformation can be described. First, the shale to sand ratio describes the sand - shale distribution across the fault, thus it can be theorized that it is a clay indicator in fault zone. Shale Gouge Ratio (SGR) is the responding indicator for clarifying the shale or clay material that slipped past the sample point of faults.

The formula for calculate SGR is:

$$SGR = \frac{\sum(V_{cl} \times \Delta z)}{Throw} \quad (1)$$

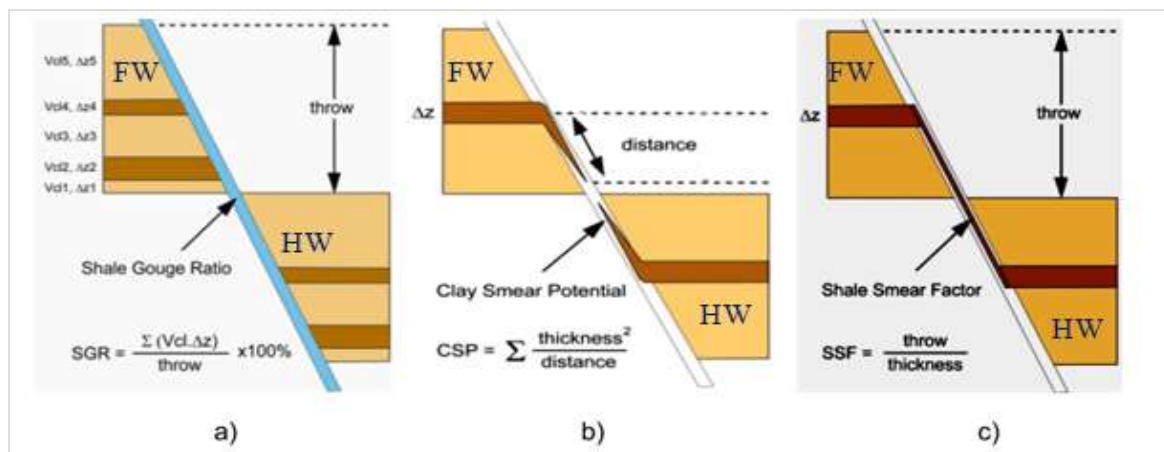


Figure 1. Different methods for predicting fault zone's clay content. (a) Shale Gouge Ratio (SGR), Yielding et al., 1997; (b) Clay Smear Potential (CSP), Bouvier et al., 1989; Fulljames et al., 1996; (c) Shale Smear Factor (SSF), Lindsay et al., 1993.

In Figure 1, there are different methods to predict fault zone's clay content: Shale Gouge Ratio (SGR), Clay Smear Potential (CSP), and Shale Smear Factor (SSF). SGR focus on the total Vclay stacking on each point, while CSP and SSF only used the thickness of the fault, and either the distance of each point or the throw length of each point accordingly. Each methods have a slightly different approach towards the sand-shale distribution, but based on the underlying formula of each method, researchers can see that SGR might be superior due to the Vclay variable because it is the direct variable contribute to the sand-shale ratio.

However, since the SGR indicator is considered a quantitative approach, fault seal analysis needs to incorporate qualitative approach into consideration. Outcrop studies show that while predicting clay smear one must consider certain controlling factors like clay bed thickness, number of clay beds present and fault throw (Kaldi, 2008). Shear type smears decrease in thickness with distance from clay source layer. Abrasion smears are eroded with greater fault throw. Multiple clay source beds can combine to produce more continuous clay smear (Yielding et al., 1997). SGR can be analyzed using triangle juxtaposition diagrams in Petrel software.

There are several processes that produce fault deformation zones with significantly reduced porosity and permeability: disaggregation, cataclasis, clay mixing, clay smearing, and fault zone cementation. Each of the processes can be identified by shale ratio content and depth.

In Figure 2, after calculating the SGR of each point across the fault, the Across Fault Pressure Difference (AFPD) can be plotted, which consist of the formula in Figure 2 and compare with the Seal envelopes for increasing burial depth, if the data point is above the envelope, the fault can be said to be sealed.

In Figure 3a, the heave, throw, and angle can be visually defined as variables representing characteristics of a fault. Fault zone thickness value shall be taken from Figure 3b plot after considered the thickness and displacement, with the typical of t_f either $\frac{D}{66}$ if the displacement is larger than 1 m, or $\frac{D}{170}$ if the displacement is smaller than 1 m.

2.2. Juxtaposition and Triangle - diagram

Juxtaposition diagrams can show the lithological juxtapositions of foot wall and hanging wall along the fault and determine whether the fault seal is due to lithological juxtapositions or due to the fault rock itself (Sahoo et al., 2010). One of the most popular juxtaposition diagrams is the 'Triangle-type diagram' developed by Knipe (1997) which provides a quick-look standalone 1D fault seal analysis tool using the well curves (Badleys, 2005). The 'Triangle-type diagram' is made of the V_{shale} log, Shale beds, SGR ratio along the depth of wells and throw distance. This method assumes that the fault throw is constant vertically down the fault, and the stratigraphy having a layer-cake shape.

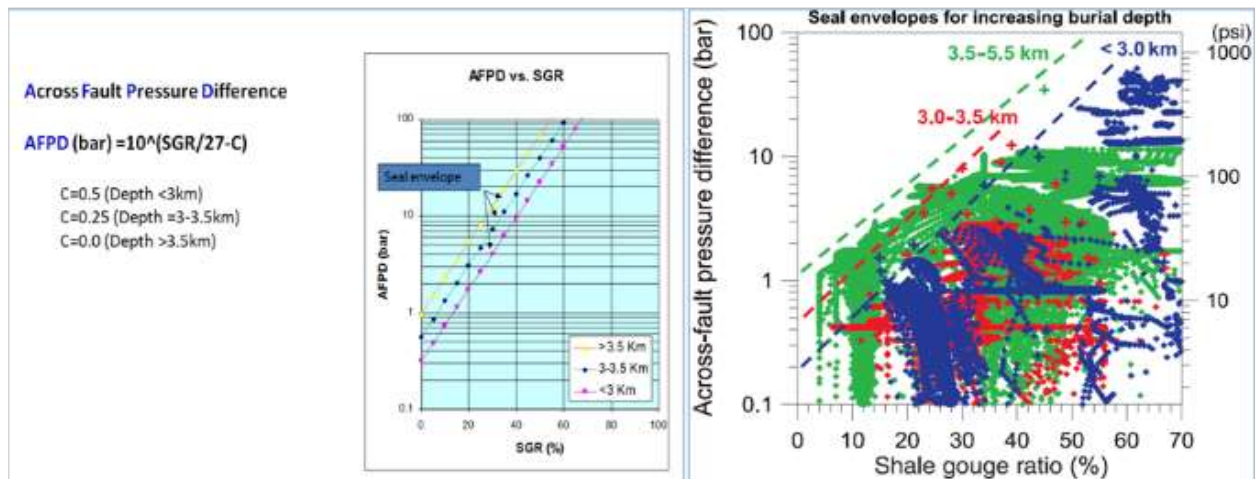


Figure 2. Across fault pressure difference with depth.

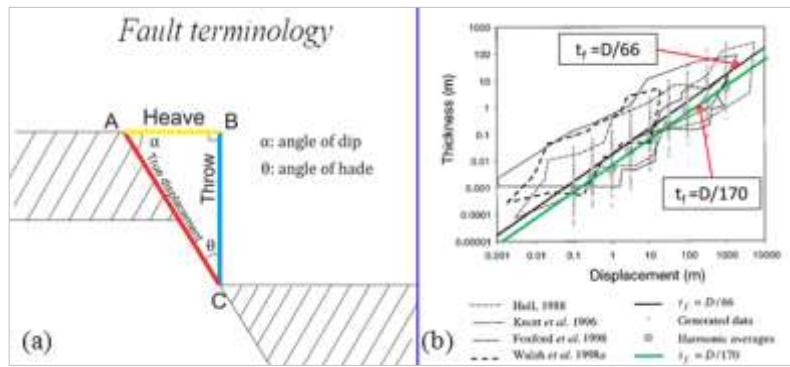


Figure 3. Fault terminology (a) and Fault thickness-displacement relationship based on outcrop data (Manzzochi et al., 1999).

The higher the value of SGR, the greater probability that the fault is sealed. Typically, the value of SGR can be quickly interpreted as the following: at SGR < 20%, normally associated with cataclastic fault gouge which the fault is not sealed; at SGR between 20÷40%, it is associated with phyllosilicate framework and some clay smear fault rocks, and the fault seal capacity is poor and retarded to fluid flow (Sahoo et al., 2010); at SGR from 40÷60%, the fault is moderate sealed and is associated with clay smear; for SGR > 60% the fault may have a considerable chance that it is completely seal.

2.3. Reactivation

Analysis in-situ stress field and fault geometry to know the likelihood of reactivation of faults and associated seal breach, which involves across fault pressure difference (AFPD).

2.4. Fault zone thickness, permeability, and transmissibility (TM)

Fault zone thickness: Figure 3 illustrates the relationship between fault zone thickness and fault displacement. As we can see, for the displacement > 1 m the formula should be:

$$t_f = \frac{D}{66} \quad (2)$$

Since displacement < 1 m are rarely represented in simulation models, we would not use it for history matching later (Manzzochi et al., 1999; Freeman et al., 2008).

Fault zone permeability from SGR: in this study, we consider 3 methods for predicting fault

zone permeability: Manzzochi et al. (1999); Jolley et al. (2007) and Sperrevik et al. (2002).

Manzzochi et al. (1999) proposed a formula which calculates fault zone permeability based on fault displacement and SGR:

$$\log k_f = -4SGR - \frac{1}{4} \log(D)(1 - SGR)^5 \quad (3)$$

Jolley et al. (2007) published multiple curves for SGR-fault permeability relationship, each curve differs based on depth of burial. All these curves have the general formula:

$$k_f = a \times SGR^{-b} \quad (4)$$

In which: k_f - fault permeability in mD; SGR - shale gouge ratio; a & b - constants. This method is more advanced than the Manzzochi et al. (1999) method since it incorporates the maximum burial depth parameter. Different burial depth represents different degrees that diagenesis has on fault seal potential, generally the deeper the more sealing. One artifact of this formula is that fault permeability approaches infinity when SGR approaches zero, so the permeability needs to be limited by the average permeability of the host rock. With Jolley et al. (2007) method, fault permeability values generally vary from zero mD up to 1mD, and much less values higher than 1mD. Fault TM values vary wildly between 0 and 1, most of point from 0 to 0.15. The Jolley et al. (2007) method gives lower permeability and TM values than the Manzzochi et al. (1999) and Sperrevik et al. (2002) methods. The difference from Manzzochi et al. (1999) method is due to the incorporation of maximum burial depth, which is

a representation of the influence of diagenesis on the faults' sealing potential

Sperrevik et al. (2002) calculate fault zone permeability based on depth at time of deformation in addition to maximum burial depth.

$$k_f = a_1 \exp - \left(a_2 V_f + a_3 z_{max} + (a_4 z_f - a_5)(1 - V_f)^7 \right) \quad (4)$$

$$a_1 = 80000, a_2 = 19.4, a_3 = 0.00403, a_4 = 0.0055, a_5 = 12.5$$

In which k_f - fault permeability in mD; V_f - fault clay content (which is approximated by SGR); z_{max} - maximum burial depth in m; z_f - depth at time of deformation in m. The time at deformation depth represents the influence of cataclasis on fault zone porosity reduction: the deeper the fault at the time of faulting, the more significant the cataclasis processes are, therefore the better the sealing potential. The Sperrevik et al. (2002) method generally gives the lowest fault permeability than the other two methods.

Fault transmissibility multiplier (TM): is a value between 0 and 1 which represents how much the faults impeded flow in the simulation grid (Badleys, 2005; Manzocchi et al., 1999). TM value of 1 means the fault has no effect on flow, while TM value of 0 means the fault is completely sealing. In this study, fault TM is calculated for each cell-to-cell juxtaposition across faults automatically. To calculate fault TM, we need permeability and thickness of fault zone, and permeability and geometry of cellblocks on both side of the fault (Figure 4).

As the name suggests, a multiplier modifies the transmissibility across the fault based on the

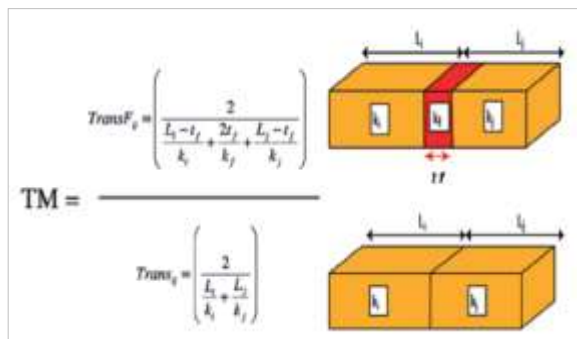


Figure 4. Fault transmissibility multiplier (TM) calculation (Jolley et al., 2007).

fault permeability, the grid permeability, the fault thickness, and the grid cell size. A low TM does not indicate a low permeability - rather it indicates that the fault has much lower transmissibility than the adjacent grid cells (so fluid flow will be retarded by the fault). When interpreting flow properties across the fault, it is best not to use the TM - this is only for input into the simulator. The better option is to look at the flow indicators - the Effective Cross-Fault Permeability and Effective Cross-Fault Transmissibility.

3. Application on Oligocene sandstone reservoir, Tay Ho field

3.1. Workflow

3D dynamic fault sealing capacity modelling workflow for simulation history matching involves the following steps (Figure 5):

- First, we would use the 3D geological model that has been approved with faults and horizon for the study area, with 3D grid containing lithological and Vclay values using facies and petrophysical modeling methods. Using this 3D geological model, fault properties can be extracted such as juxtaposition, displacement, SGR.

- Second, we would predict the fault zone thickness, and then calculate the fault zone permeability by three suitable methods. Third, complementing those methods by cementation factor that measures the cementation effect due to diagenesis.

- Finally, by applying the fault zone permeability results from different methods, we would decide the optimized result by both history matching in dynamic model and cementation factor, combine with reasonable geological theory.

Since the 3D dynamic fault sealing capacity modeling needs to be closely resemble the historical production profile, the steps above need to be put in an iteration until the simulated production profile match the actual one, so if the flow analysis does not reach a satisfying answer, researchers need to use the previous answer as a baseline and redo from the first step.

3.2. Data and research methods

3.2.1. Database

Figure 6 represents some background information of the Tay Ho field: the 3D seismic first acquired by PCVL in 2002, and processing in PSDM in 2005 and finally HFCBM in 2011 and GI in 2012. Each seismic processing area can be seen in the Figure 6.

In Lower Oligocene, Tay Ho field, the

following data will be used in this study:

+ Seismic data:

- 3D HFCBM processing.
- Seismic interpretation included structural map and fault polygon, fault stick, map of reservoirs.

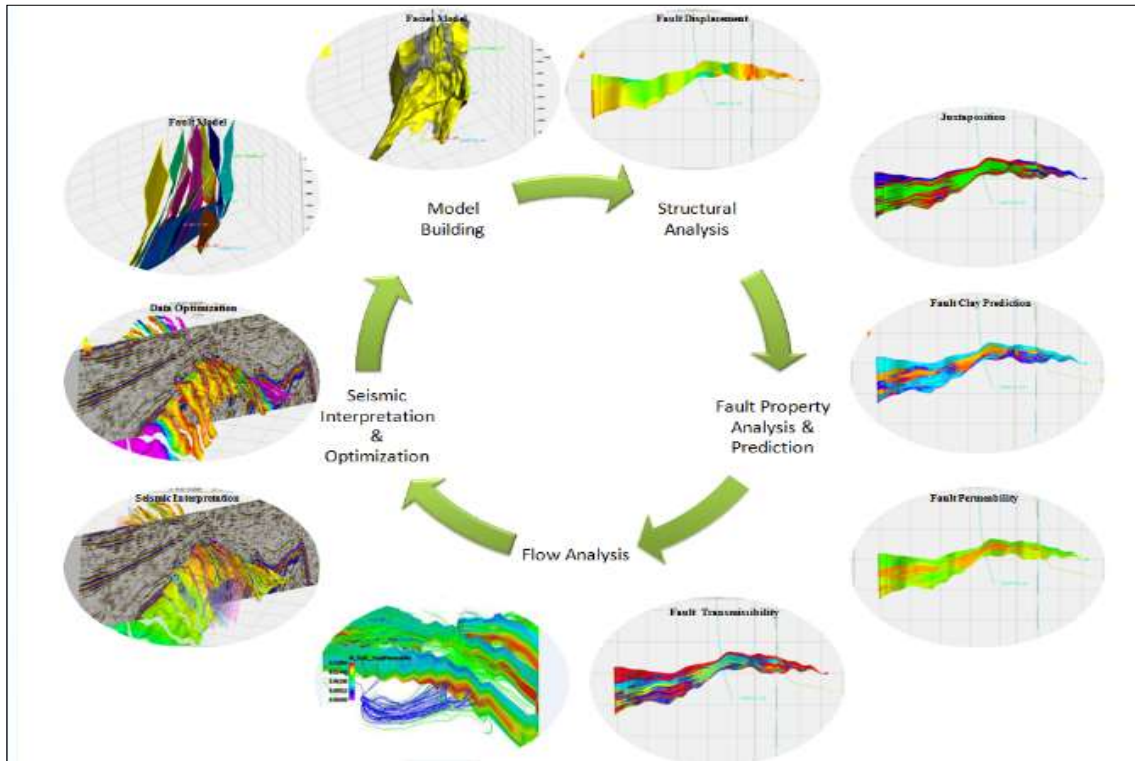


Figure 5. 3D dynamic fault sealing capacity modelling workflow.

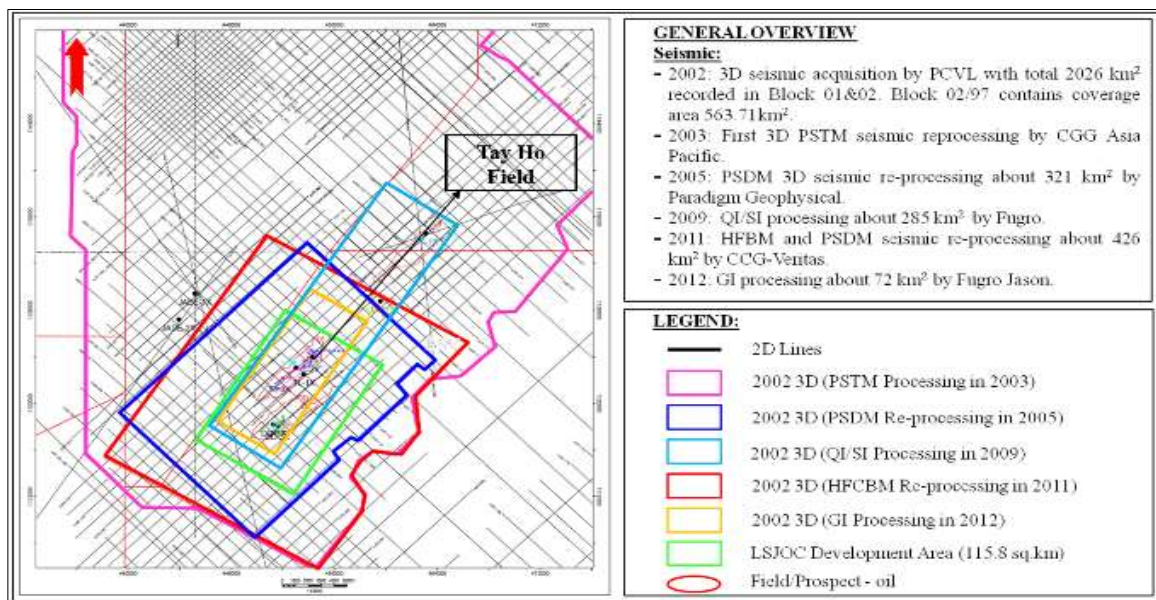


Figure 6. Tay Ho Field Location - Seismic Survey and Well Locations.

- Seismic inversion cube: Well data: 3 exploration wells (TH-1X, 2X) and 5 production wells (TH-3P, 5P, 7P, 9XPST, 10XP).

+ Well data: 3 exploration wells (TH-1X, 2X) and 5 production wells (TH-3P, 5P, 7P, 9XPST, 10XP)

- Well log data including wireline log, composite log, mudlog, masterlog, DST, PTA, petrographical analysis, geochemistry analysis, biostratigraphy analyses data.

- TH-3X conventional core data.

+ 3D geological and dynamic models.

3.2.2. Application in Oligocene sandstone reservoir

3.2.2.1. Oligocene reservoir geological model

The 3D geological model is made of cell dimension 50x50x1.2 m. The cell thickness of the fine scale model (1.2 m) is reasonable given our sand thickness distribution analysis which can capture thinnest sand layer. The lithological and Vclay models have been approved for the development plan. The lithological cutoff is $V_{cl} \leq 0.4$ and $Phie \geq 0.09$ for reservoir rocks and vice versus.

There are in total 33 faults that have been interpreted in fault stick, fault model was built on fault set, which interpreted and exported from software and was quality checked in Petrel software. The Oligocene fault set has NE-SW direction normal faults and one sub-East-West (sub-E-W) strike-slip fault. Most of faults within Oligocene sequence have NE-SW and sub-latitude trends, forming series of parallel NE-SW horsts/half-horsts and grabens/half-grabens. Major faults play a main role of dividing the study

area into 06 segments such as F4, F5, F6, F7, F8, F10, F11a, F11b, F12, F13 and F22 will be selected for fault seal capacity analysis (Figure 7).

3.2.2.2. Well juxtapositions

1D well triangle juxtaposition diagram provides a quick-look standalone 1D fault seal analysis tool using the well curves. Well juxtaposition allows assessing the impact of faults and fault throws on stratigraphy models. Among 08 exploration and production wells, three exploration wells (1X, 2X, 3X) and 10 XP which are low deviated profile will be selected for triangle juxtaposition analysis:

TH-1X triangle juxtaposition (Figure 8) analysis result indicated that the sand-sand juxtaposition window is about 30 m with $SGR < 0.3$, this suggests the fault near to well to be leaking one if fault throw is less than 30 m.

TH-2X triangle juxtaposition (Figure 9) analysis is shown in the depth interval 2093÷2158 mSS are mainly sand on sand juxtapositions are found. SGR is calculated in this interval and within maximum throw limit most of the sand-on-sand juxtapositions show $SGR < 0.3$ with few showing $SGR 0.2 \div 0.35$ in the lowermost sand unit. This suggests the fault to be a leaking one if fault throw is less than 80 m.

TH-3X triangle juxtaposition (Figure 10) analysis is shown in the depth interval 2117÷2170 mSS are mainly sand on sand juxtapositions are found. SGR is calculated in this interval and within maximum throw limit most of the sand-on-sand juxtapositions show $SGR < 0.3$. This suggests the fault to be a leaking one if fault throw is less than 60 m.

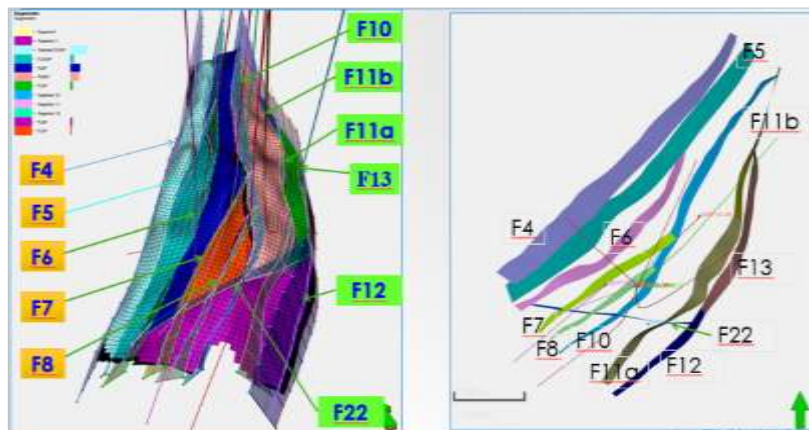


Figure 7. Structural model of Oligocene reservoir, Tay Ho field.

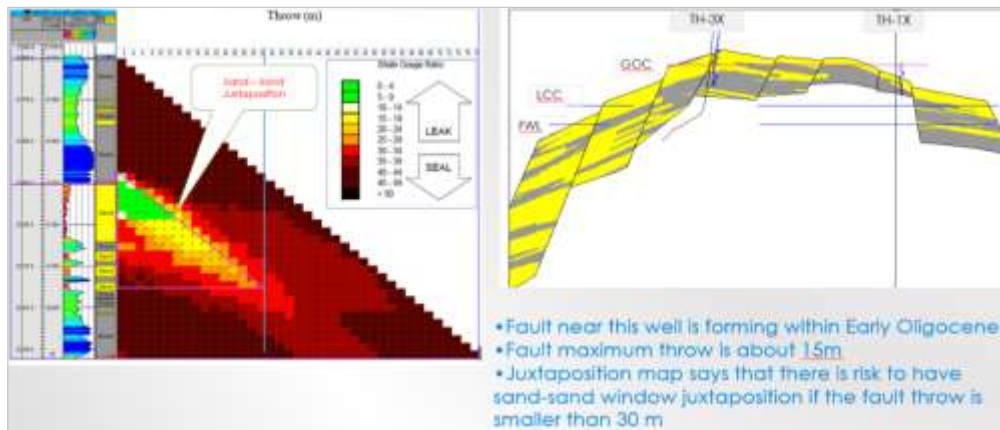


Figure 8. SGR Triangle diagram for TH-1X.

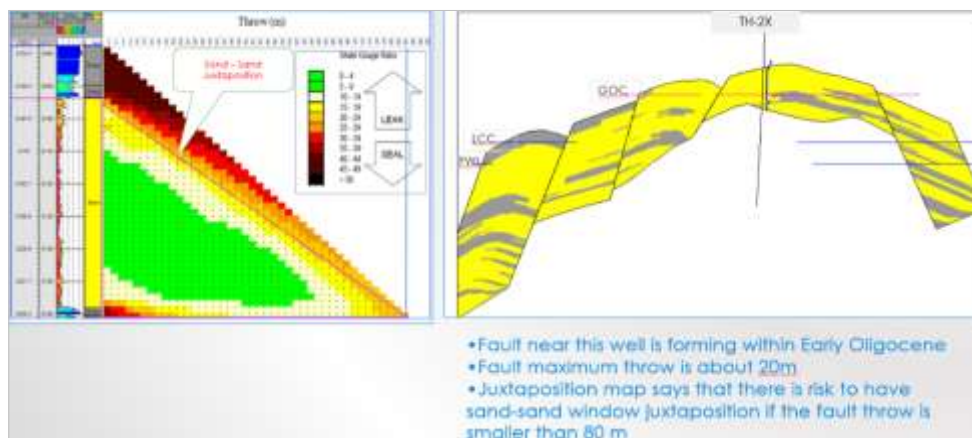


Figure 9. SGR Triangle diagram for TH-2X.

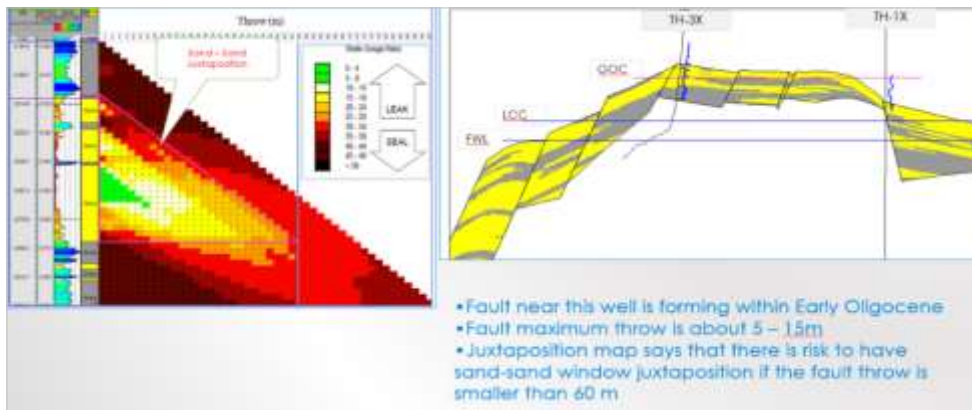


Figure 10. SGR Triangle diagram for TH-3X.

TH-10XP triangle juxtaposition analysis (Figure 11) is shown in the depth interval 2160÷2215 m and 2270÷2320 mSS are mainly sand on sand juxtapositions are found. SGR is calculated in this interval and within maximum throw limit, most of the sand-on-sand juxtapositions show SGR < 0.3 This suggests the

fault to be a leaking one if fault throw is less than 80 m.

3.2.2.3. 3D fault clay from seismic inversion

Based on results from seismic inversion carried out in 2012, Vclay frequency volume was generated from reservoir sand probability. 3D

fault clay was generated by mapping 3D Vclay volume data to fault. Above FWL @ 2283, 3D fault plan clay is quite low vary from 10÷30% @ sand-sand juxtaposition (Figure 12).

3.2.2.4. 3D fault juxtaposition model

The subsurface structural framework is critical to the first-order control of the potential connections across fault surfaces, visualized in Allan Diagrams.

In the analysis of the seal across the intra-reservoir fault, we consider the juxtaposition of the hanging-wall and footwall stratigraphy against the fault using a two-dimensional analysis having the stratigraphy projected onto a vertical plane through the average strike of the fault. This two-dimensional analysis first described by Allan (1989) is a simple technique to evaluate the lateral changes in stratigraphic juxtaposition

across the fault surface. Allan (1989) is a simple technique to evaluate the lateral changes in stratigraphic juxtaposition across the fault surface.

The hanging-wall and footwall horizons intersecting the fault surface (horizon cutoffs) are derived from the seismic interpretation. The well-log tops are tied to the seismic horizons and the stratigraphic section shortened and expanded between the hanging-wall and footwall cutoffs along the fault surface. The litho-facies model is used to sand distribution sand bodies in hanging-wall and footwall.

Figure 13 shows cross section from TH-1X to TH-10XP and TH-7P to TH-10XP across segments indicated that almost sand-sand juxtaposition above LCC and FWL, whilst fault displacement is general to small.

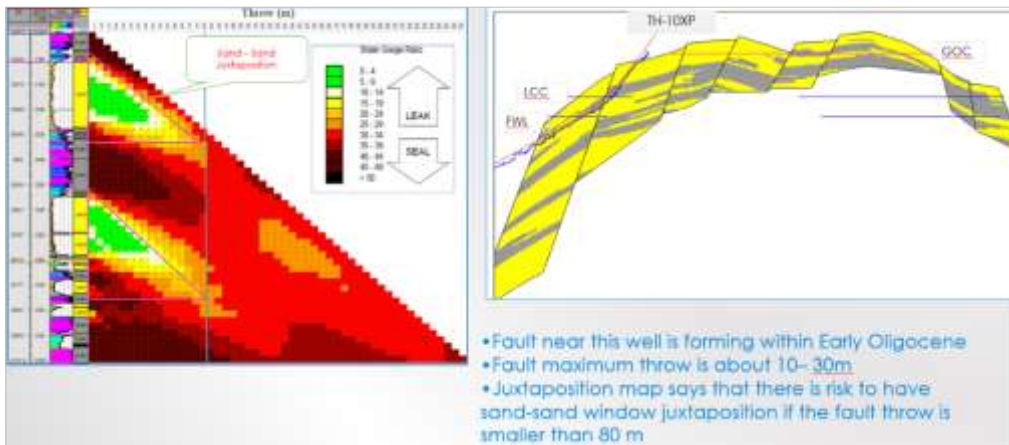


Figure 11. SGR Triangle diagram for TH-10XP.

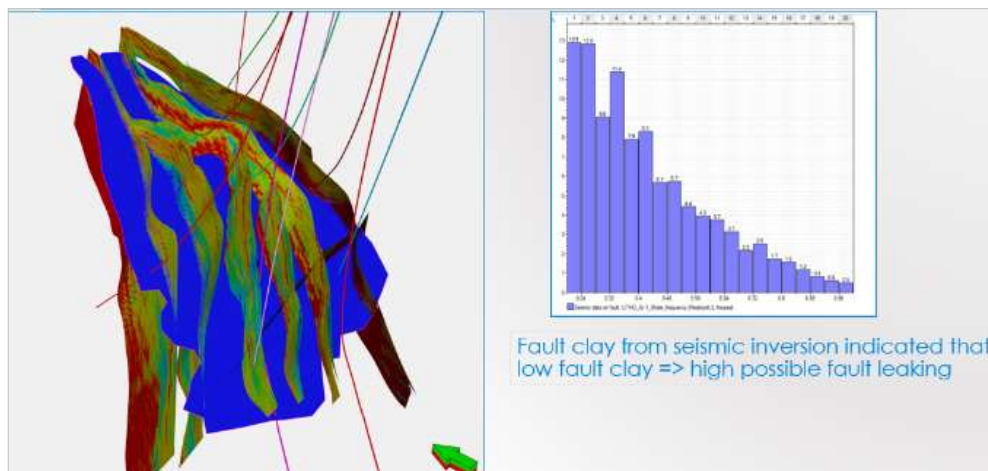


Figure 12. 3D Fault Clay model from Seismic inversion.

Figure 14 shows fault juxtaposition of the reservoir & non-reservoir facies performed before evaluating shale gouge ratio. The juxtaposition of non-reservoir against non-reservoir is color-coded as blue. Reservoir-reservoir juxtaposition is colored green, and Reservoir-non-reservoir is red. This color schemes allows to quickly identify the fault throws that deliver Reservoir-reservoir or reservoir-non-reservoir juxtaposition for the formation of interest. Figure 14 shows that the juxtaposition of the Oligocene with reservoirs - non-reservoir juxtaposition and thus a potential leakage of the fault.

3.2.2.5. 3D fault clay prediction model from SGR and smear model

Classification of fault rocks is fundamentally based on their composition (Fisher and Knipe,

1998), and hence SGR can be thought of as a predictor of fault-rock types for simple fault zones. Fault rocks with phyllosilicate content < ca. 15÷20% are typically catalases or disaggregation zones, those with >ca. 40% phyllosilicate are clay = shale smears, and intermediate compositions are sometimes referred to as clay-matrix gouges (Gibson, 1998) or phyllosilicate-framework fault rocks (Fisher and Knipe, 1998).

The process of building 3D fault clay model, as known as SGR model, consists of two components: 3D V_{clay} model and Smear model. SGR model clarifies the shale distribution in faults and can be used to determine the sealing abilities. Frisstad et al. (1997), Yielding et al. (1997) and Freeman et al. (1998) created multiple approach on how one can build SGR model, but the process is similar. First, the assumption needed to be made is that material across the fault gouge

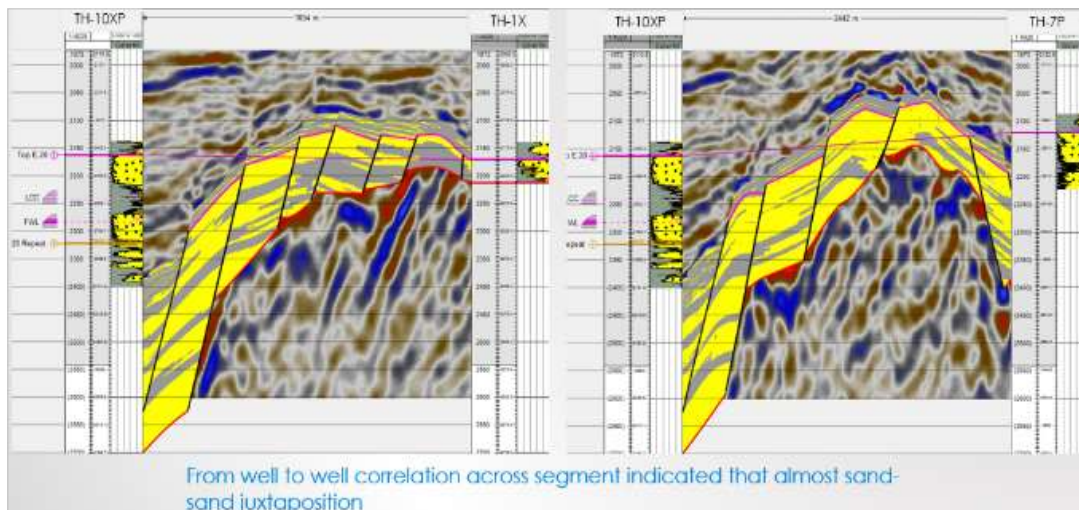


Figure 13. Well Correlation across Segments indicated sand-sand juxtaposition.

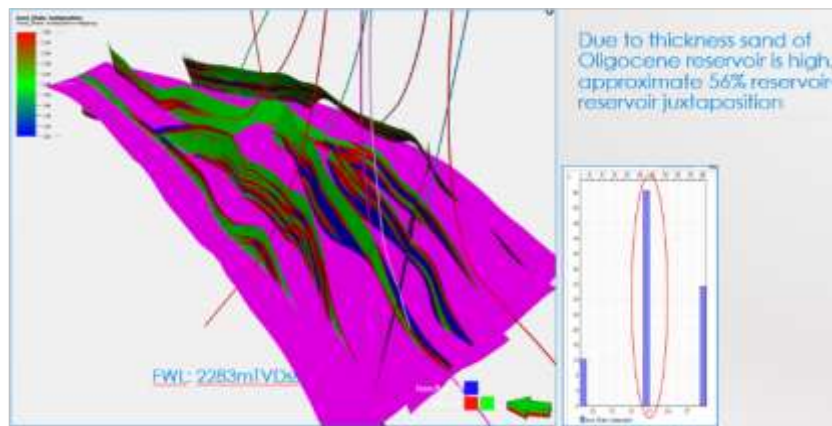


Figure 14. 3D Fault Juxtaposition Model.

should be more or less the same trend on the wall rocks in the slipped interval. Secondly, the model should include the information about the net content of shale-clay in the volume of rock that has slipped past that point on the fault in each point, which Petrel modelling it as “cell”. Classification of fault rocks is fundamentally based on their composition (Fisher and Knipe, 1998), and hence SGR can be thought of as a predictor of fault-rock types for simple fault zones. Fault rocks with phyllosilicate content < ca. 15÷20% are typically catalases or disaggregation zones, those with >ca. 40% phyllosilicate are clay = shale smears, and intermediate compositions are sometimes referred to as clay-matrix gouges (Gibson, 1998) or phyllosilicate-framework fault rocks (Fisher and Knipe, 1998).

Figure 15 demonstrated SGR model and 3D fault clay prediction from SGR. The SGR of all faults of Oligocene model in reservoir-reservoir juxtaposition are low from 10÷25% which is quite consistent with well data and V_{clay} model from seismic inversion.

Other fault-seal algorithms, for example Clay Smear Potential (CSP): (Bouvier et al., 1989; Fulljames et al., 1996) and Shale Smear Factor (SSF): (Lindsay et al., 1993), attempt to model the development of clay or shale smears from clay or shale beds within the faulted sequence CSP was created after the observation of ductile clays whereas SSF was created after the study of lithified shales. Naruk and Handschy (1997), suggested that SGR is superior to CSP because of

the distinct characteristic of CSP which heavily bias to ductile clay. As we analyzed and studied, it is heavily implied that although there are multiple methods for determining the fault seal capacity, they are all pointed to the sand-shale distribution of every point across the fault, just the clay interested was different, and the geologist should use each method with a grain of salt and the catagenesis characteristic of each area that was being studied.

The clay smear factor of Tay Ho Oligocene reservoir defines the ratio of the displacement distance to the continuous shale bed thickness against the fault that can occur before the smear breaks down, clay will smear when V_{shale} property is greater than a cut-off value of 40%. (Figure 16). A clay smear factor of 3 means that a continuous shale bed can be displaced by three times its original thickness before that smear breaks down.

3.2.2.6. Across fault pressure difference

Observations of sealing faults in the subsurface provide first-hand evidence of the ability of fault zones to support pressure differences. Simple recognition of different hydrocarbon contacts across an area of reservoir juxtaposition shows that there is static pressure support, at or below the sealing capacity of the fault zone. In this study, Tay Ho Lower Oligocene depth is from 2000÷3000 mTVDss, therefore seal-failure envelopes are line less than 3 km with $C = 0.5$. The cross plot between AFPD & SGR (Figure 17) of all faults in model drop onto above seal

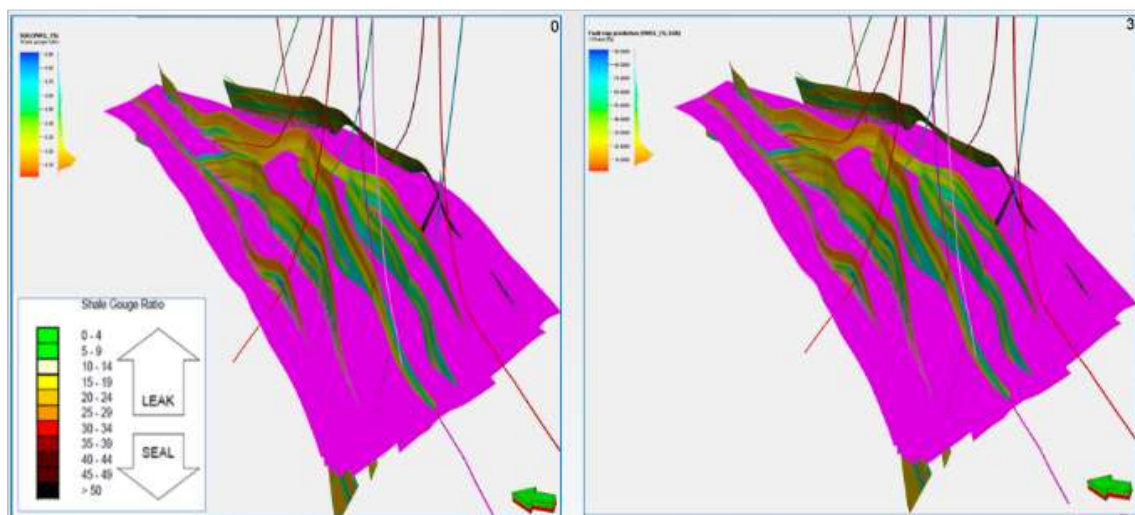


Figure 15. 3D Fault SGR and Fault clay prediction from SGR.

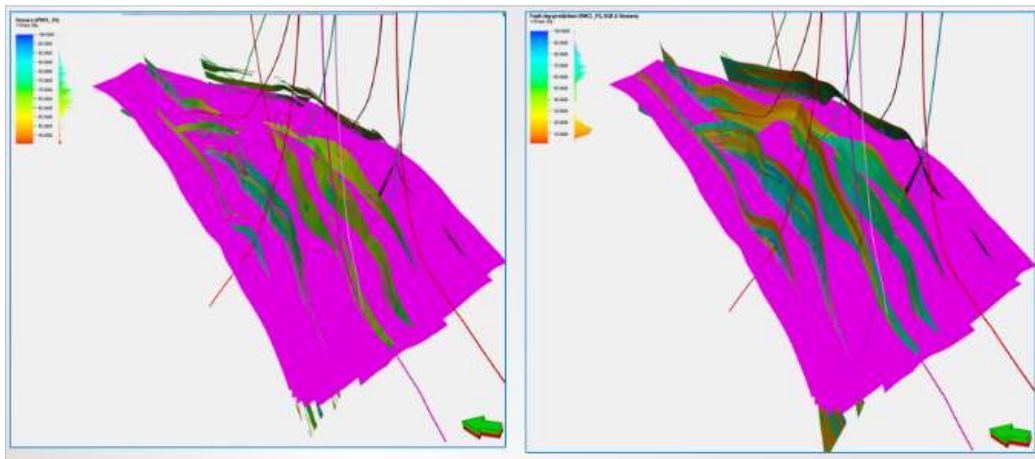


Figure 16. 3D Fault Smear and Fault clay prediction from SGR&Smear.

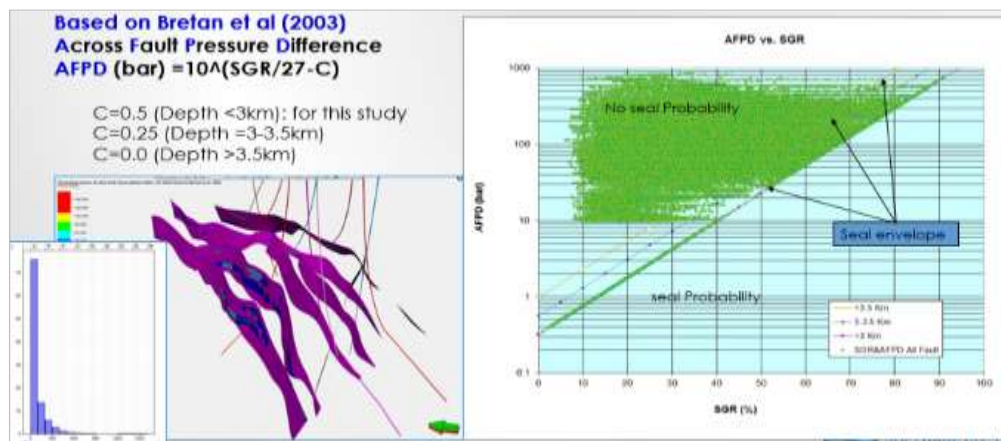


Figure 17. AFPD vs SGR.

envelope, AFDP vary from 10÷1000 bar. This observation supports the idea that the area below the envelope represents static fault seal, whereas the area above the envelope represents seal failure of fault rocks of variable capillary entry pressure. Otherwise, there would not be such consistency between the sample data plotted using measured phyllosilicate content and the subsurface data plotted using SGR.

3.2.2.7. Fault throw, fault displacement, fault heave

Fault throw is calculated as the vertical horizon offset between the hanging wall and the footwall sides of the fault for the different horizons. Figure 18 illustrated fault throw of Oligocene model, the result indicated that fault throw is from 5÷20 m, rarely 30÷40 m.

Fault displacement is calculated down the fault surface and takes account of the variation in the fault surface form. Calculations are conducted

down average fault dip. Fault displacement of Tay Ho Oligocene model is also from 5÷40 m, rarely 40÷60 m (Figure 19)

The fault heave (lateral horizon offset from the footwall and hanging wall of the fault) is over the fault surface. Calculations are conducted down average fault dip. Fault heave of Tay Ho Oligocene model is also from 5÷20 m, rarely 20÷40 m (Figure 20).

3.2.2.8. 3D fault zone thickness model

Fault zones comprise portions where two or more slip surface bound volumes of deformed rock and portions where the entire displacement is accommodated on single slip surfaces. The thickness of the fault zone is defined as either the separation between the outermost slip surfaces minus the thickness of undeformed lenses, or the thickness of slip-surface itself in lacuna. For Tay Ho Oligocene model, to estimate fault zone

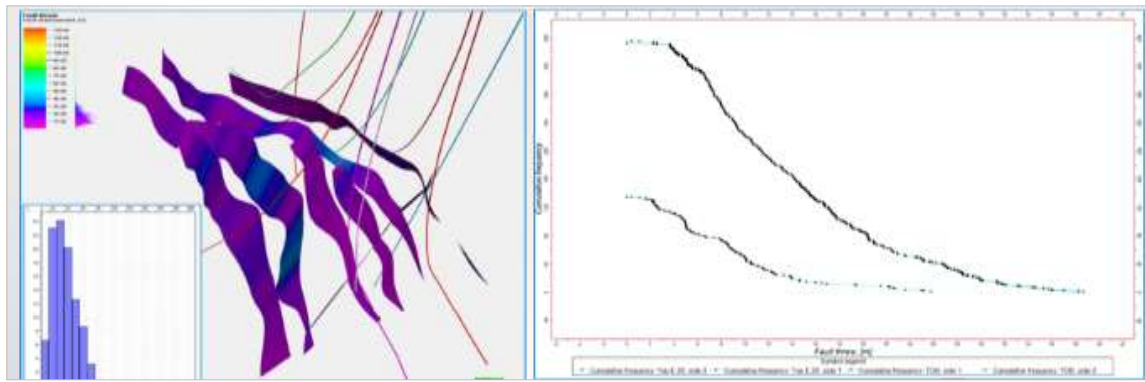


Figure 18. 3D Fault throw model.

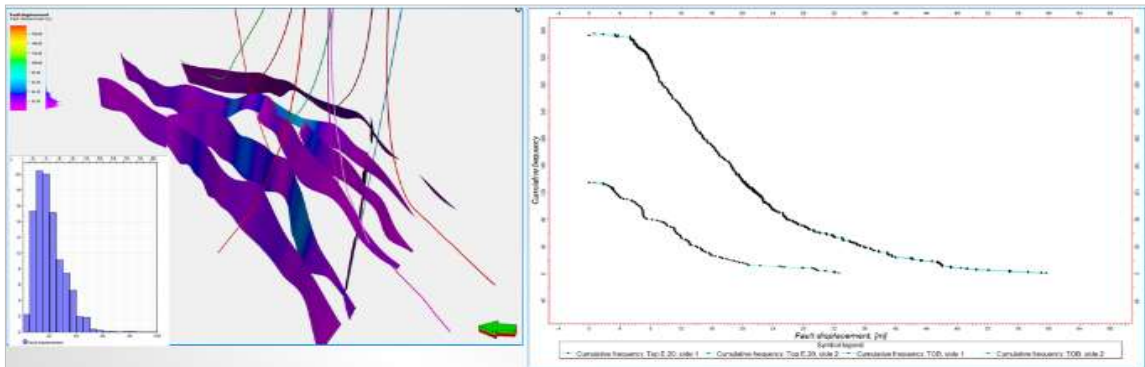


Figure 19. 3D Fault displacement model.

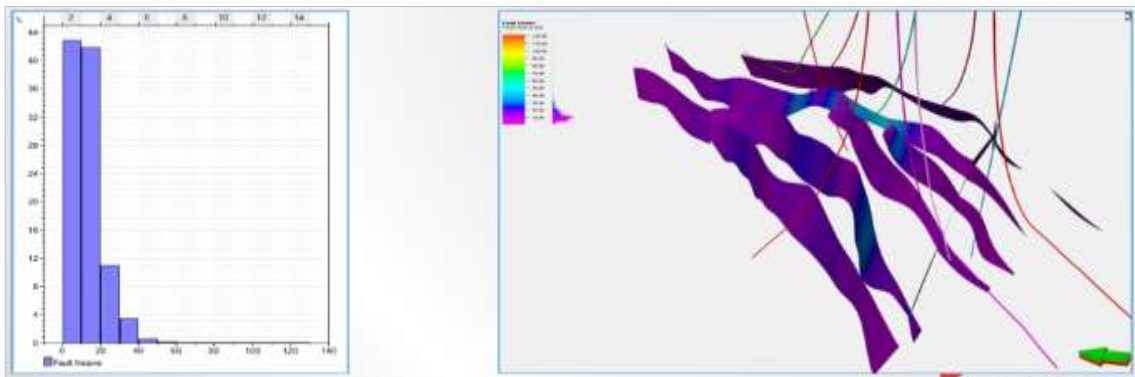


Figure 20. 3D Fault heave model.

thickness, the $t_f = D/66$ has been applied to define a median thickness value, and standard deviation for $\log(t_f)$ of 0.9 to define a log-normal thickness distribution. The displacement to thickness ratio of 66 better represents faults with displacement are greater than 1 m, while fault with displacement is less than 1 m are rarely represented in simulation models. The thickness of all faults in Oligocene model are vary from 0.1÷3 m (Figure 21).

3.2.2.9. 3D Fault permeability and transmissibility

Jolley et al. (2007), Manzocchi et al. (1999), and Sperrevik et al. (2002) were applied to predict fault zone permeability with results are presented in Figures 22÷26, respectively.

3.3. Validate fault seal model against observed data

After conducting fault seal analysis, fault transmissibility multipliers (TM) are exported to Blocks A-Tay Ho Oligocene simulation model for history matching. The simulation model has a

dimension of 50x50x1.2 m, and the history match is designed for the period from 2014 to present. The key matching parameter is pressure data during the match period for TH-3P, TH-2P, TH-7P, TH-9XP, TH-10XP. After the first run, methods further optimization.

In addition to fault validation through simulation history matching, DST analysis results are also used to support our fault seal model.

The results based on Sperrevik et al. (2002) show the best matching, especially at built-up period of TH-2P, the results based on Jolley et al. (2007) method comes in second, and the Manzocchi et al. (1999) method has the worst match. Thus, the Sperrevik et al. (2002) method is chosen for further matching optimization. (Figure 27).

3.4 Optimization of chosen methods and evaluating the influence of faults on simulation results

To improve the quality of history matching and to investigate the effect from the faults have

on simulation results; faults will attempt closed to see the well-by-well performance. This is geologically reasonable due to poor shorting, lithofacies changing and cementation can significantly enhance the sealing potential.

To evaluate the influence of faults on simulation results, the fault will be closed in order that the transmissibility is of zero. The results show clear effects of fault seal on pressure matching. When closing F10, TH-3P & TH-5P show significant improvement matching even at interference and dropped pressure. Closing F11, TH-7P and TH-9XP have under history pressure, trying to reduce transmissibility of F11 produces an immediate improvement, therefore F11 is not fully sealed. Similar F11, closing F6 will make under history pressure at wells and reducing trans of F6 will improvement history matching.

F22 fault is right-lateral strike slip fault, therefore displacement on E sequence is not clear. In simulation validate, closing or opening this fault did not impact on the simulation result.

Comparison with build-up interpretation,

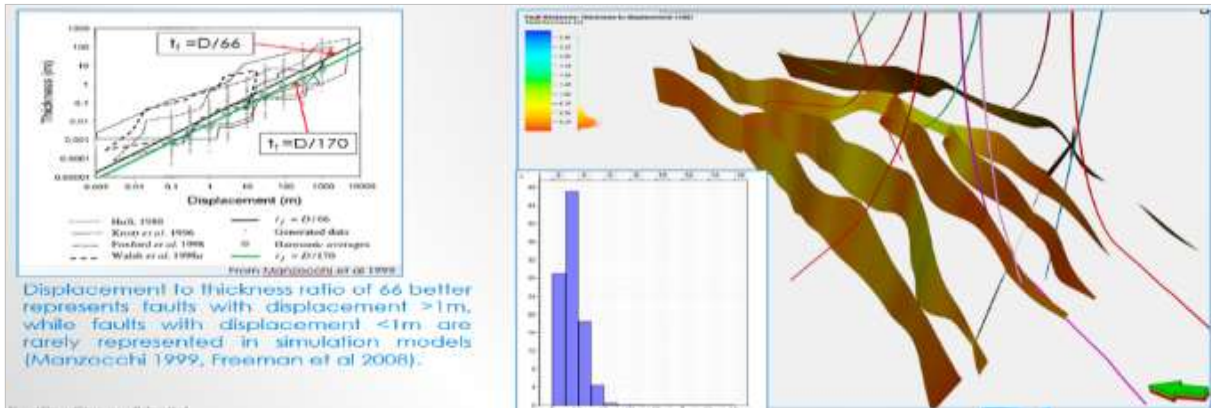


Figure 21. 3D Fault thickness model.

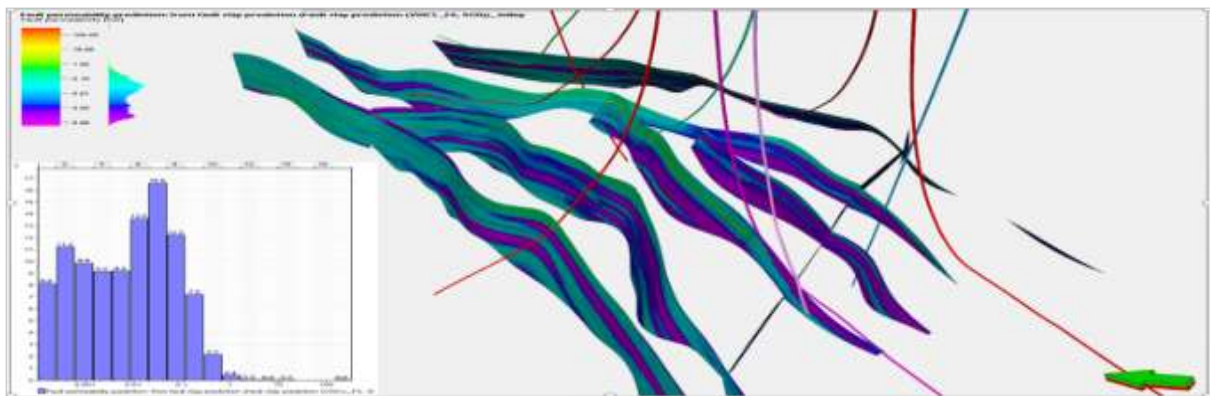


Figure 22. 3D Fault Perm based on Jolley et al. (2007).

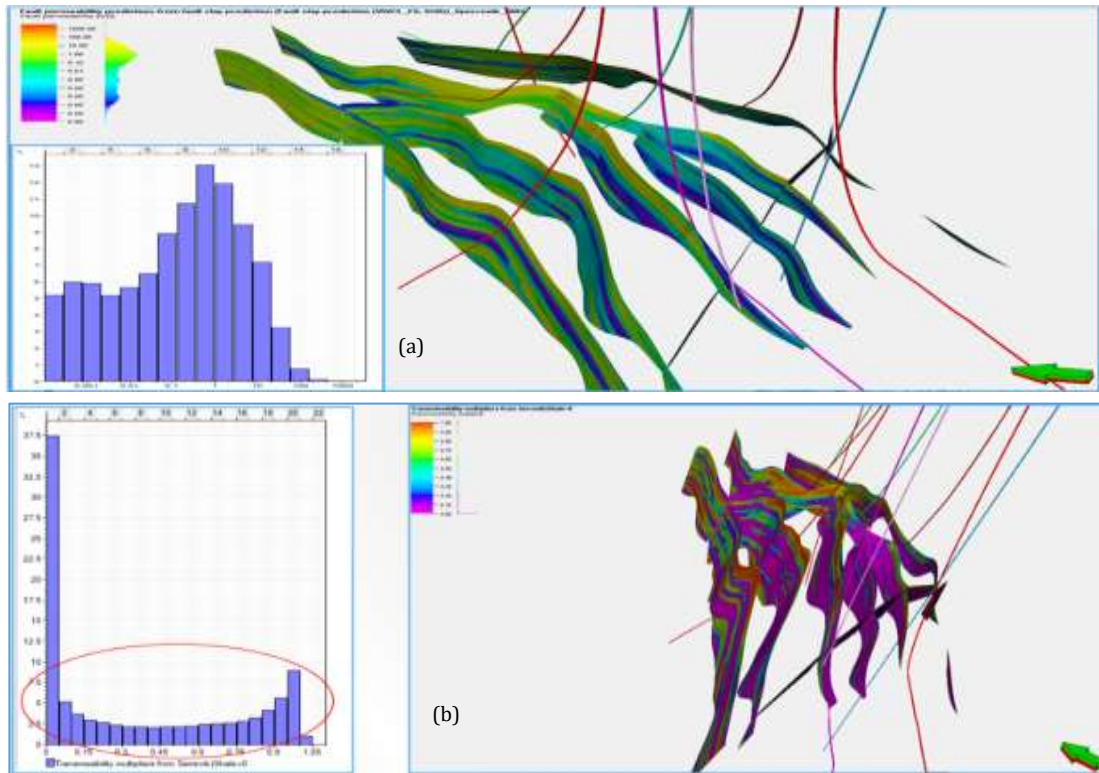


Figure 23. (a, b) 3D Fault Permeability based on Sperrevik et al. (2002).

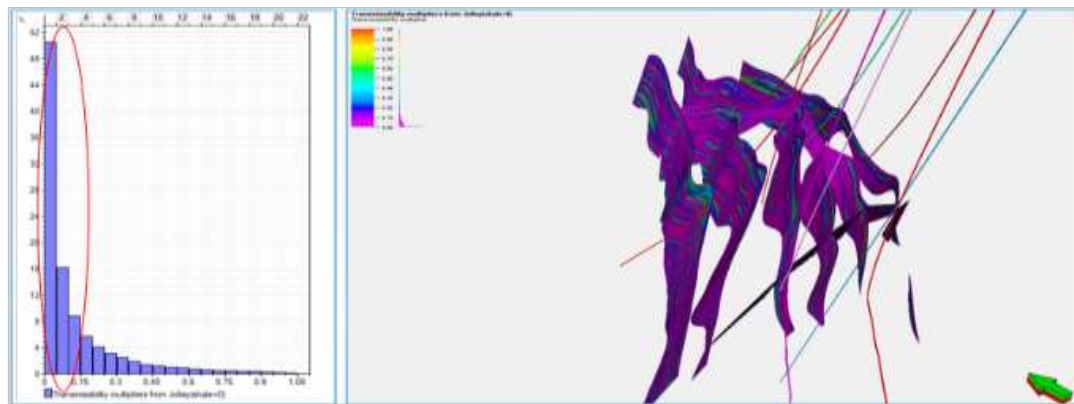


Figure 24. 3D Fault Transmissibility based on Jolley et al. (2007).

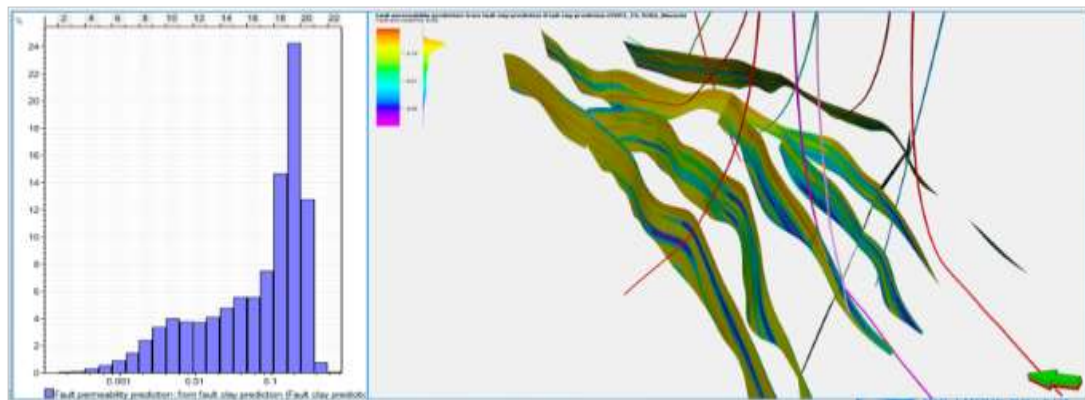


Figure 25. Fault Permeability based on Manzocchi et al. (1999).

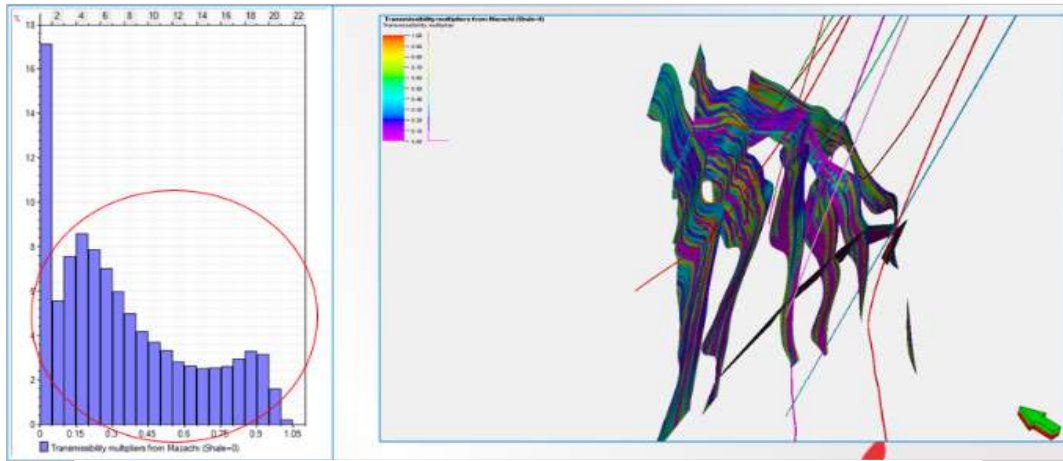


Figure 26. Fault Transmissibility based on Manzocchi et al. (1999).

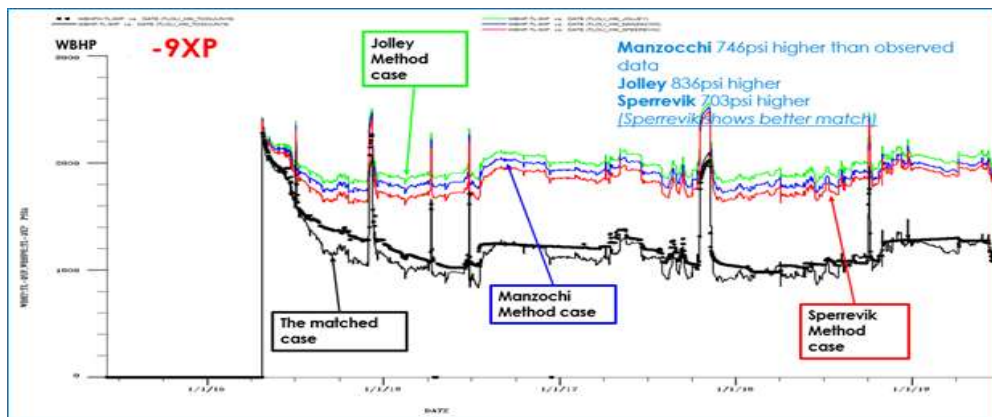


Figure 27. Simulated bottom hole pressure for well TH-9XP using three methods.

TH-5P and TH-10 are possibility interference and TH-7P & TH-9XP are the same status. Therefore, it can be concluded that F6 and F11 are not fully sealed.

Overall, the Sperrevik et al. (2002) method produces a good match and consistency with build-up interpretation.

4. Conclusion

Out of the three fault permeability prediction methods, the Sperrevik et al. (2002) method produces the best history matching. The Manzocchi et al. (1999) method does not consider diagenesis therefore predicts low sealing potential for the faults and has the worse history match. Jolley et al. (2007) method considers diagenesis and has better history match, but the predicted permeability is still too open.

We have achieved a good match with the Sperrevik et al. (2002) method with still manage

to be geologically reasonable, and the results were validated by history matching and build up and interference test. Based on this method, the fault sealing analysis result are:

- Faults F10, F8, F22 are closed, and contribute directly to the compartmentalization of the reservoir.
- Faults F7, F11 transmissibility is reduced.
- Fault F6 transmissibility is increasing.

As in any study, uncertainties always existed. In Tay Ho Oligocene, there is only one conventional core in TH-3X well and the seismic data of this project is quite poor on the flank, thus it leads to some uncertainties. First is fault picking which is heavily dependent on seismic credibility. Second is the SGR calculation, which V_{shale} is served as an input. V_{shale} relies strongly on core calibration when using XRD analysis, thus when the number of conventional cores is limited, the confidence in V_{shale} interpretation has typically included uncertainty.

Contribution of authors

Hung Viet Vu and Dong Duc Nguyen - are mentors that guide the whole study; Gia Phuoc Phan - drafted the manuscript; Vu Minh Le and Hai Hoang Ninh - support and secondarily draft the manuscript. All authors read and approved the final manuscript.

References

- Allan, U. S. (1989). Model for hydrocarbon migration and entrapment within faulted structures: *AAPG Bulletin*, 73, 803-811.
- Badleys, (2005). *Reference manual*, Trap Tester, p. 4.1-4.12.
- Bouvier, J. D., Kaars-Sijpesteijn, C. H., Kluesner, D. F., Onyejekwe, C. C., & Van der Pal, R. C. (1989). Three-dimensional seismic interpretation and fault sealing investigations, Nun River Field, Nigeria. *AAPG bulletin*, 73(11), 1397-1414.
- Fisher, Q. J., and Knipe, R. J. (1998). Fault sealing processes in siliciclastic sediments. Geological Society, London, Special Publications, Vol. 147, 117 - 134.
- Freeman, B., Yielding, G., Needham, D. T., & Badley, M. E. (1998). Fault seal prediction: the gouge ratio method. *Geological Society, London, Special Publications*, 127(1), 19-25. 10.1144/GSL.SP.1998.127.01.03.
- Freeman, S., Harris, S. & Knipe, R. (2008). *Fault seal mapping - Incorporating geometric and property uncertainty*. Geological Society, London, Special Publications. 309. 5-38. 10.1144/SP309.2.
- Fristad, T., Groth, A., Yielding, G. Freeman, B. (1997). Quantitative fault seal prediction: A case study from Oseberg Syd. *Norwegian Petroleum Society Special Publications*, 107-124.
- Fulljames, J. R., Zijerveld, L. J. J., Franssen, R. C. M. W., Ingram, G. M., and Richard P. D. (1996). Fault seal processes, in Norwegian Petroleum Society, eds., *Hydrocarbon seals-importance for exploration and production (conference abstracts)*. Oslo, Norwegian Petroleum Society, p. 5.
- Gibson, R. G. (1998). Physical character and fluid-flow properties of sandstone-derived fault zones, in M.P. Coward, T.S. Daltaban, and H. Johnson, eds., *Structural geology in reservoir characterization Geological Society(London) Special Publication 127*, p. 83-97.
- Jolley, S. J., Dijk, H., Lamens, J. H., Fisher, Q. J., Manzocchi, T., Eikmans, H., & Huang, Y. (2007). Faulting and fault sealing in production simulation models: Brent Province, northern North Sea. *Petroleum Geoscience*, 13, 321-340.
- Kaldi, J. (2008). Evaluating reservoir quality, seal potential and net pay: *GEO India pre-conference training*. 27 June - 1, July 2016, Lagos.
- Lindsay, N. G., Murphy, F. C., Walsh, J. J., & Watterson, J. (1993). Outcrop studies of shale smear on fault surfaces. *International Association of Sedimentologists Special Publication 15*, 113-123.
- Manzocchi, T., Walsh, J. J., Nell, P., & Yielding, G. (1999). Fault transmissibility multiplier for flow simulation models. *Petroleum fGeoscience*, 5, 53-63.
- Naruk, S. J., and Handschy, J. W. (1997). Characterization and prediction of fault seal parameters: empirical data (abs.): AAPG Hedberg Research Conference on "Reservoir scale deformation: characterisation and prediction", Bryce, Utah.
- Sahoo, T. R., Tuser, R., Nayak, S., Sankar, S., Senapati, S., & Singh, Y. N. (2010). Fault seal analysis: a method to reduce uncertainty in hydrocarbon exploration, Case study: northern part of Cambay Basin. In *8th Biennial International Conference and Exposition on Petroleum Geophysics* (1-9). India. DOI: 10.13140/2.1.2575.3285.
- Sperrevik, S., Gillespie, P. A., Fisher, Q. J., Halvorsen, T., & Knipe, R. J. (2002). Empirical estimation of fault rock properties. In *Norwegian Petroleum Society Special Publications* (11, 109-125). Elsevier.
- Yielding, G., Freeman, B., & Needham, D. T. (1997). Quantitative fault seal prediction. *AAPG Bulletin*, 81, 897-917.